Molecular Solvation and Mobility in Polymer/Liquid Interphases. A Fluorescence Study on Polystyrene−Poly(ethylene glycol) Microbeads

B. Lehr,[†] H. -J. Egelhaaf,[†] H. Fritz,[‡] W. Rapp,[§] E. Bayer,[‡] and D. Oelkrug*[,†]

Institute of Physical Chemistry and Institute of Organic Chemistry, University of Tübingen, Auf der Morgenstelle 8, D-72076 Tübingen, Germany, and Rapp Polymere GmbH, Ernst-Simon-Strasse 9, D 72072 Tübingen, Germany

Received April 16, 1996; Revised Manuscript Received August 6, 1996[⊗]

ABSTRACT: Porous microbeads of low cross-linked polystyrene (PS) grafted with poly(ethylene glycol) chains (PEG) are labeled at the free chain ends with 3-(1,6-diphenyl-1,3,5-hexatrienyl)propionic acid (DPH-PA) and 1-(dimethylamino)naphthalene-5-sulfonic acid (DANS), which probe the polarizability, polarity, and viscosity of their environments. The beads are investigated in a series of pure liquid phases and in acetonitrile/water mixtures by electronic absorption and steady state as well as time-resolved fluorescence spectroscopy. The extent of solvation in the polymer/liquid interphase is characterized from spectral shifts by introducing a solvation fraction which quantifies the relative amount of polymer and liquid in the solvation shell. The rotational mobility of DPH-PA is derived from time-resolved fluorescence anisotropy measurements. Depending on the liquid phase, the rotational correlation times vary strongly between $\tau_R = 500$ ps and 100 ns. The shortest τ_R-values are found in liquids which are able to solvate both the fluorophore and the polymer, e.g. toluene and acetonitrile. Long correlation times are observed in the presence of aliphatic hydrocarbons, which do not solvate the bead and therefore cannot penetrate into the polymeric frame, and in presence of water, which solvates PEG but not PS and DPH. In contrast, water is able to weakly solvate DANS chemically bound to the polymeric frame.

I. Introduction

Polymeric microbeads are gaining increased significance as chemical microreactors, chromatographic separation chambers, or easy to handle analytical detection systems. Depending on the type of application, the beads have to be chemically modified at the surface or in the bulk. In the latter case, the gaseous or liquid environment must be able to penetrate into the beads, forming a dispersion on the molecular scale between the stationary polymer and the mobile liquid. This type of dispersion is called a chemical "interphase". Good candidates for stationary phases are low cross-linked polymeric backbones, e.g. polystyrene (PS) prepared in the presence of small amounts of 1,4-divinylbenzene (DVB), which are grafted with chains of linear polymers, e.g. poly(ethylene glycol) (PEG).[1−4] The free ends of PEG can be modified with various functional y-groups. Several types of these flexible and geltype polymers ("Tentagel" ≡ TG) are available with bead diameters of $d = 10^{-3}$−1 mm.[5] Figure 1 shows schematically the polymer structure.

In order to optimize chemical reactions within the beads, it is important to know the mobility and solvation of the interphase components. In this paper we contribute to the characterization of these quantities using the technique of fluorescence probing. A small amount of y-groups (typically 0.1%) will be chemically linked to a fluorophore which reacts sensitively to, for example, the dielectric constant, refractive index, viscosity, free volume, or pH of the environment. From transition energies, polarization, and decay kinetics of fluorescence it will be possible to gain information about the primary solvation shell and the rotational diffusion of the fluorophore as well as the transport capacity of the liquid

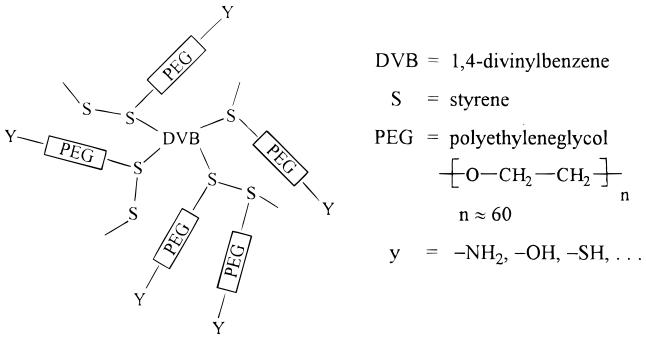

Figure 1. Building blocks of Tentagel.

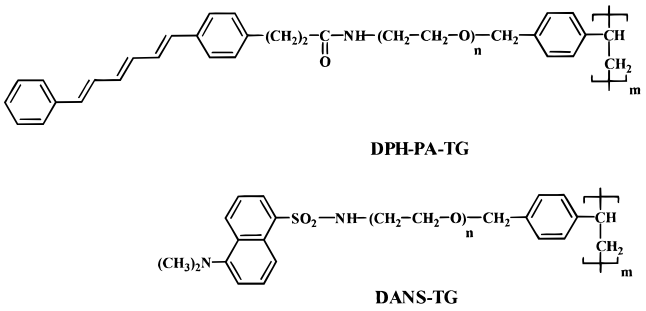

Figure 2. Structure of DPH-PA and DANS linked to Tentagel.

phase. The fluorophores are selected with regard to high fluorescence quantum yields, high intrinsic fluorescence anisotropies, and long fluorescence lifetimes in order to be able to probe also slow rotational correlation times in the range of $\tau_R = 10^{-8}$−10^{-7} s. Since, in addition, the fluorophores should discriminate between different types of solvents, we linked 3-(1,6-diphenyl-1,3,5-hexatrienyl)propionic acid (DPH-PA) and 1-(dimethylamino)naphthalene-5-sulfonic acid (DANS) as nonpolar and polar chromophores, respectively, via y = NH_2 to TG (cf. Figure 2). Both chromophores are well-established mobility and polarity probes for cell membranes, polypeptides, or synthetic copolymers.[6−16] The

[†] Institute of Physical Chemistry, University of Tübingen.
[‡] Institute of Organic Chemistry, University of Tübingen.
[§] Rapp Polymere GmbH.
[⊗] Abstract published in *Advance ACS Abstracts,* October 15, 1996.

S0024-9297(96)00558-X CCC: $12.00 © 1996 American Chemical Society

Table 1. Solvation Fractions (x_S) and Rotational Correlation Times $\tau_{R,i}$ of DPH-PA−TG/Liquid Interphases

liquid phase	solvation fraction, x_S	swelling volume/mL/g	rotational correlation times $\tau_{R,1}$/ns	$\tau_{R,2}$/ns	A_1[a]	A_2[a]	$\langle\tau_R\rangle$/ns
dichloromethane	0.71	5.1	0.30 ± 0.06	0.82 ± 0.16	0.63	0.37	0.5
acetonitrile	0.68	5.1	0.39 ± 0.07	1.60 ± 0.35	0.68	0.32	0.8
toluene	0.68	5.7	0.61 ± 0.09	2.7 ± 0.4	0.62	0.38	1.4
methanol	0.54	4.3	0.79 ± 0.07	5.4 ± 0.7	0.67	0.33	2.3
ethanol	0.52	2.1	1.7 ± 0.2	10 ± 3	0.72	0.28	4.0
diethyl ether	0.13	1.7	–	27 ± 5 (se)			
cyclohexane	0.04	1.7	–	35 ± 9 (se)			
water	0.12	4.3	–	85 ± 10 (se)			
dry	0	1.7					

[a] A_i are the relative amplitudes of the double exponential anisotropy decay analysis, and $\langle\tau_R\rangle$ the average rotational correlation times. se = single exponential analysis.

advantages of these probes are their high intrinsic fluorescence anisotropies, approaching in DPH the theoretical limit of $r_0 = 0.4$; their long fluorescence lifetimes, ranging from $\tau_F \approx 2-30$ ns; their spectral positions of absorption and fluorescence, depending on the polarizability or polarity of the environment; and the very small overlap of fluorescence and absorption spectra, which reduces the probability of undesired concentration depolarization.

II. Experimental Section

Sample Preparation. DANS-Cl (FLUKA), DPH-PA (Molecular Probes), and TG microspheres[5] of $d = 90$ μm particle size were used as received. The swelling volume of TG microspheres (Table 1) is the volume of the sedimented, swollen beads in a specified liquid in milliliters per gram. Details of the swelling volume determination are given elsewhere.[17] The functionalization of TG (0.3 mmol/g total capacity, y = NH_2) with DANS was performed by shaking 2 g of the beads in a dry dichloromethane solution of 1 mg DANS-Cl for 2 h at room temperature. The functionalization of TG with DPH-PA was performed by shaking 0.5 g of the beads in a solution of 0.3 mg of DPH-PA (esterified with hydroxybenzotriazol) at room temperature overnight. After filtration, the beads were thoroughly washed in dichloromethane, methanol, and diethyl ether and dried in vacuum. The filtrate showed no fluorescence, indicating the complete linkage of the fluorophores to the polymer. The quantity of the used fluorophores was chosen to cover 0.1−1% of all available amino groups. The average fluorophore concentration was determined by UV-absorption spectroscopy. Typical concentrations for fluorescence probing were $c = 10^{-4}$ mol of DPH-PA/L of TG and 10^{-3} mol of DANS/L of TG.

Fluorescence Measurements. Functionalized TG microspheres (≈1 mg) were suspended in organic solvents of spectroscopic grade. The suspensions were stirred in commercial cuvettes to avoid sedimentation. Fluorescence spectra and steady state anisotropy measurements were performed on a Spex Fluorolog 222 spectrometer equipped with two calcite polarizers. The wavenumbers of excitation and fluorescence maxima were determined by a polynomial fit of the spectral peak regions and yielded an accuracy of $\Delta\nu_{max} \leq 10$ cm^{-1}. Fluorescence decay times were obtained by the single photon counting method[18,19] using a Thyratron-controlled nanosecond flashlamp as excitation source. Time-resolved anisotropy decay measurements were performed at the Center for Fluorescence Spectroscopy in Baltimore, MD by single photon counting. As excitation source a cavity-dumped, frequency-doubled pyridine 1 dye laser was used ($\lambda_{ex} = 360$ nm, fwhm = 7 ps, repetition rate 3 MHz). A microchannel plate photomultiplier (Hamamatsu R2809) provided an instrument response function near 60 ps. Rotational correlation times obtained from steady-state anisotropy and fluorescence decay measurements were calculated by applying the Perrin equation.[20] Average fluorescence decay times $\langle\tau_F\rangle$ were obtained from a double exponential decay analysis $I_F(t) = A_1 \exp(\tau_1/t) + A_2 \exp(\tau_2/t)$ and $\langle\tau_F\rangle = (A_1\tau_1^2 + A_2\tau_2^2)/(A_1\tau_1 + A_1\tau_1)$. Anisotropy decay curves were obtained by fitting $r(t) = D(t)/S(t)$, where

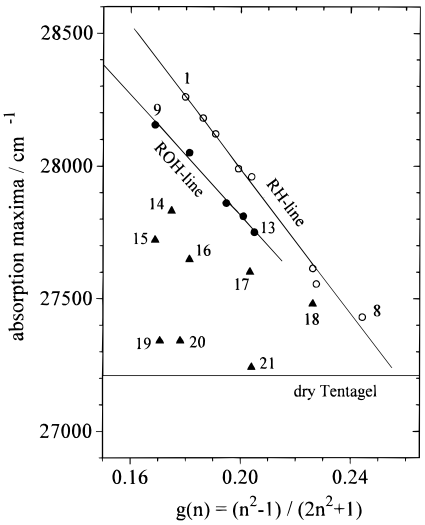

Figure 3. Positions of the $S_2(0-1)$-maxima of DPH-PA in solvents of different refractive index n and of DPH-PA−TG/liquid interphases. Open circles denote hydrocarbon (RH) solutions: *n*-pentane (1), *n*-hexane (2), *n*-heptane (3), *n*-decane (4), cyclohexane (5), toluene (6), benzene (7), polystyrene (8). Full circles: alcoholic (ROH) solutions: methanol (9), ethanol (10), butanol (11), hexanol (12), octanol (13). Triangles denote TG/liquid interphases: liquid = acetonitrile (14), methanol (15), ethanol (16), dichloromethane (17), toluene (18), water (19), diethylether (20), cyclohexane (21).

$D(t) = I_{vv}(t) - I_{vh}(t)g$ and $S(t) = I_{vv}(t) + 2I_{vh}(t)g$. Details of anisotropy decay data analysis can be found in refs.[20−22] The scaling factor $g = I_{hv}/I_{hh}$ was determined for each decay experiment.

III. Results and Discussion

Transition Energies of the Probe Molecules. DPH-PA−TG/Liquid Interphases. The red-shift of $\pi-\pi^*$-transitions of DPH-PA can be used to probe the *polarizability* of the environment.[22,23] The amount of red-shift depends on the oscillator strength (f) of the fluorophore and the polarizability function of the solvent, $g(n)$, which is usually approximated by the Onsager relation $g(n) = (n^2-1)/(2n^2+1)$,[23] where n is the refractive index of the environment. In DPH, $f(S_0 \rightarrow S_2)$ is much higher than $f(S_0 \rightarrow S_1)$ so that the S_2-band shifts strongly with $g(n)$, whereas the position of S_1 is almost unaffected in absorption and in fluorescence. Several authors[24−26] find satisfactory linearity between the S_2-maxima in very different types of solvents and the Onsager relation. However, linearity can be significantly improved if only one type of solvent is considered. Figure 3 presents our results for a series of hydrocarbons including polystyrene and for a series of aliphatic alcohols. The linearity within each of both

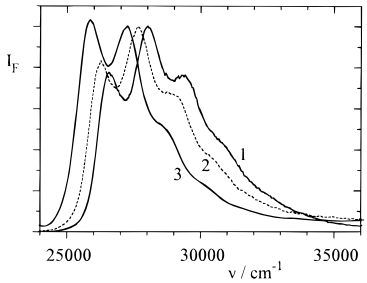

Figure 4. Fluorescence excitation spectra of DPH-PA in ethanol (1), of the DPH-PA−TG/ethanol interphase (2), and of the DPH-PA−TG/nitrogen interphase (3).

series is much more perfect than the overall linearity, indicating a systematic alcoholic polarity or H-bonding shift in addition to the dominant polarization shift.

The S_2-maxima, ν, of DPH-PA chemically bound to TG are determined by TG itself and by the influence of the liquid phase in which TG is dispersed. Figure 4 compares the absorption spectrum of DPH-PA dissolved in ethanol with the absorption spectra of the fluorophore chemically bound to TG in an environment of ethanol and gaseous nitrogen. The spectrum is red-shifted with the growing influence of the polymer. The low energetic limit of S_2, ν_{TG}, is reached in the absence of a liquid phase. This limit is drawn in Figure 3 as a straight line parallel to the abscissa. In the presence of "bad" solvents like aliphatic hydrocarbons, diethyl ether, or water, the S_2-maximum stays close to its low energetic limit independent of the refractive index of the solvent. In the presence of "good" solvents like dichloromethane, acetonitrile, or toluene, the maximum shifts toward the position of the freely dissolved probe, ν_{Solv}, but never reaches this high energetic limit. In order to quantify the environment of DPH in the interphase, we introduce the solvation fraction $x_s = (\nu - \nu_{TG})/(\nu_{Solv} - \nu_{TG})$, which becomes zero for the probe completely attached to TG and unity for the probe fully solvated by the mobile liquid phase. Table 1 summarizes x_s-values for a series of different TG/liquid interphases. "Good" and "bad" solvents result in $x_s \approx 0.7$ and $x_s < 0.1$, respectively, in general accordance with the macroscopic swelling volume of TG in the corresponding liquid (cf. Table 1). The exception is water, which is able to solvate PEG but not PS and DPH. Therefore, the transition energy of DPH-PA is almost the same as in dry TG. On the other hand, aliphatic hydrocarbons are able to solvate DPH, but the transition energy of DPH-PA is far away from ν_{Solv}, because these solvents are not able to solvate the PEG spacer and swell the bead (see the low swelling volume). Similar results are obtained from gelphase ^{13}C-NMR investigations [27] and measurements of spin−lattice relaxation times.[4]

DANS−TG/Liquid Interphases. The electronic transitions of DANS react more sensitively but also with more complexity to the environment than unsaturated hydrocarbons. Because of the resonant electron-donating dimethylamino and electron-accepting sulfonyl groups, the band positions of DANS probe mainly the *polarity* [14,28] of the environment but also *H-bonding* to n-electron pairs and *solvent reorganization* after excitation. With increasing polarity and/or H-bonding the position of the $S_0 \rightarrow S_1$-absorption shifts slightly to the blue (this is typical for *n*-electrons participating in the electron transition). Fluorescence, however, shifts strongly to the red since the dipole moment of DANS is much bigger in the excited state than in the ground state and therefore intramolecular charge transfer (CT)

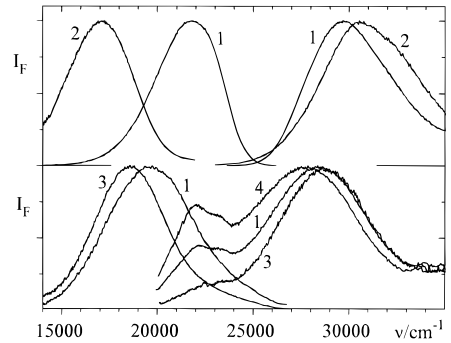

Figure 5. Fluorescence spectra (left) and fluorescence excitation spectra (right) of (upper) DANS-NH_2 in cyclohexane (1) and water (2) and (lower) DANS−TG dispersed in cyclohexane (1), acetonitrile (3), and gaseous nitrogen (4).

is facilitated with the increasing polarity of the solvent. In addition, the CT process induces solvent reorganization, which also contributes to the red-shift of fluorescence. Figure 5 compares in the upper part two extreme spectral situations of DANS dissolved once in nonpolar cyclohexane (dielectric constant $\epsilon = 2$) and once in polar water ($\epsilon = 80$). For other liquids, see Table 2. The lower part of Figure 5 presents spectra of the interphases DANS−TG in the environment of acetonitrile, cyclohexane, and gaseous nitrogen. The fluorescence is red-shifted in polar liquids like acetonitrile or water, but less than in free solution, which is especially valid for water (cf. Table 2). Obviously, polar liquids inclusive of water are able to solvate the fluorophore in the interphase but not as fully as in free solution. However, quantitative data similar to the solvation fraction of DPH-PA−TG (cf. Table 1) cannot be extracted from Stokes shifts alone since part of the shift is due to solvent relaxation which is strongly hindered in the regions where DANS is chemically bound to TG.

At the red tail of S_1 the system DANS−TG produces an additional absorption band ($\nu_{max} = 22\,500$ cm^{-1}, cf. Figure 5) which we assign to aggregated $(DANS)_x$. The assignment is based on a similar band which appears in p-(dimethylamino)benzonitrile adsorbed on porous metal oxides[29] and which, as in DANS−TG, disappears by reducing the loading with fluorophore. Since, at given loading, the intensity of the preband reacts on the nature of the environment, this effect can be used to probe the association ↔ dissociation equilibrium of DANS in the interphase. For TG we find the following series of decreasing association tendencies: dry sample ($K_a = 7$) > dispersion in cyclohexane ($K_a = 4$) > water ($K_a = 2$) > acetonitrile ($K_a = 1$). Here K_a is the relative association constant estimated from the intensity ratios of the preband and S_1. The series is in general accordance with the solvation of DPH-PA−TG and the swelling volume. The exception is cyclohexane, which shows almost no effect on DPH but a clear though small effect on DANS. So it cannot be excluded for the moment that, due to the kinetics of synthesis, DANS and especially $(DANS)_x$ are concentrated in the outer regions of the beads interacting somewhat also with "poor" solvents whereas DPH is homogeneously distributed over the whole sphere.

Fluorescence Anisotropy in Tentagel/Liquid Interphases. Time-Resolved Fluorescence Depolarization. The kinetics of fluorescence depolarization probes the *rotational mobility* of the fluorophore in a given environment. Figure 6 presents a selection of fluorescence anisotropy decay curves of DPH-PA−TG dispersed in different liquid phases. First-order decay

Table 2. Relative Stokes Shifts $\Delta\nu$ (dry DNS-TG as reference), Average Fluorescence Lifetimes $\langle\tau_F\rangle$, Steady State Fluorescence Anisotropies $\langle r\rangle$, and Rotational Correlation Times $\bar{\tau}_R$ of DNS-TG/Liquid Interphases

liquid phase	dielectric constant, ϵ	solution of DNS amide: $\Delta\nu$/cm^{-1}	DNS-TG/liquid interphases			
			$\Delta\nu$/cm^{-1}	$\langle\tau_F\rangle$/ns	$\langle r\rangle$	$\bar{\tau}_R$/ns[a]
dry		−	0	11	b	−
cyclohexane	2.0	−600	300	13	0.31	$\rightarrow\infty$
toluene	2.4	500	600	8.9	0.03	0.9
acetonitrile	38	2200	1600	16	0.03	1.7
ethanol	24	2500	1500	13	0.05	2.4
water	80	5000	1200	15	0.17	17

[a] Data based on the intrinsic anisotropy of $r_0 = 0.32$. [b] Not measurable because of fluorescence depolarization by multiple light scattering within one bead.

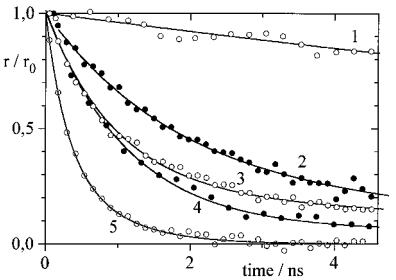

Figure 6. Fluorescence anisotropy decay curves of DPH-PA−TG dispersed in ether (1), ethanol (2), methanol (3), toluene (4), and dichloromethane (5). All curves are normalized to unity at t = 0. Circles are experimental data, and solid lines are exponential (1) and biexponential (2−5) fits.

analysis separates the systems into a wide range of rotational correlation times from $\tau_R \approx 500$ ps to $\tau_R \approx 100$ ns (cf. Table1). The shortest τ_R-values are found in acetonitrile and dichloromethane, which already have been classified by spectral band shifts (Figure 3) as "good" solvents. However, even in these solvents the correlation times are not as short as for freely dissolved DPH-PA, with $\tau_R = 180-200$ ps. Obviously, rotational diffusion of chemically bound DPH is not only determined by the fluorophore itself but also by the flexibility of the whole polymeric frame. If parts of the polymer are rigid, as is the case in an environment of aliphatic hydrocarbons, ether, or water, the correlation times will be very long.

Upon closer inspection the anisotropy decay curves in Figure 6 deviate from the exponential law. This is not very surprising since full rotation of DPH needs mobility of the PEG chains, and also of the PS backbone if DPH is not completely solvated by the mobile phase. The decay of such a complex system cannot be described analytically but can be approximated by a sum of exponentials

$$r(t) = r_0(1 - \mathrm{f(s)})\sum \mathrm{A}_i \mathrm{e}^{-t/\tau_{\mathrm{R},i}} \quad (1)$$

Here $\tau_{R,i}$ is the partial rotational correlation time of the system, A_i its relative amplitude ($\sum A_i = 1$), r_0 the intrinsic fluorescence anisotropy, and *f(s)* a depolarization factor accounting for multiple scattering of the excitation and/or fluorescence radiation. For times longer than 10 ps this factor adopts constant values of $f(s) \approx 0.05-0.2$, depending on the size and optical inhomogeneity of the beads. Since anisotropy decay curves are by far not as accurate as fluorescence decay curves, it makes little sense to extract more than two exponentials from the experiment. The results of biexponential analysis are summarized in Table 1. Very tentatively we assign the short and the long correlation times to rotational diffusion of the whole system ($\tau_{R,1}$) and of the TG frame ($\tau_{R,2}$). The $\tau_{R,2}$-component corresponds well with the swelling volume and also with the solvation fraction of Table 1. For ether, cyclohexane, and water, no short decay component could be found. This means that DPH is closely attached to TG and not solvated. Whether the long decay of $\tau_{R,2} \approx 100$ ns is really due to rotational diffusion of TG or due to concentration depolarization cannot be decided at the present stage of the investigation.

Table 3. Steady State Fluorescence Anisotropies $\langle r\rangle$, Average Fluorescence Decay Times $\langle\tau_F\rangle$, and Rotational Correlation Times $\bar{\tau}_R$ of DPH, DPH-PA, and DANS-NH$_2$ Dissolved in Highly Viscous Polymer

fluorophore/solvent	$\langle r\rangle$	$\langle\tau_F\rangle$/ns	τ_R/ns
DPH/PMMA[a]	0.38	7.9	>200
DPH-PA/PMMA[a]	0.375	6.3	>200
DPH-PA/PS	0.31	4.4	19
DPH-PA/PEG[b]	0.12	3.7	1.7
DANS-NH$_2$/PMMA[a]	0.30	15	>200

[a] Containing 5% HMDMA. [b] Molecular mass ≈3000 Da.

Steady State Fluorescence Anisotropy. This kind of investigation reduces experimental expenditure and enables convenient monochromatic excitation over a large wavelength range. Integration of (1) combines the steady state anisotropy $\langle r\rangle$ with the rotational correlation time. However, simple expressions are obtained only for identical first-order fluorescence decay times τ_F of all components with different correlation times. In this case

$$\langle r\rangle = r_0(1 - \mathrm{f(s)})\sum \mathrm{A}_i(1 + \tau_F/\tau_{\mathrm{R},i})^{-1} \quad (2)$$

Experimentally, the pseudocorrelation time ($\bar{\tau}_R$) can be extracted from steady state measurements

$$\langle r\rangle = r_0(1 - f(s))(1 + \tau_F/\bar{\tau}_R)^{-1} \quad (3)$$

For exponential anisotropy decay curves, eqs 2 and 3 become identical. For multiexponential decays and short correlation times, $\sum A_i\tau_{R,i} \ll \tau_F$, the pseudocorrelation time is approximately equal to the average correlation time $\langle\tau_R\rangle = \sum A_i\tau_{R,i}$. However, if one component decays fast and the other one very slowly because of restricted mobility of the polymer to which the fluorophore is attached, the pseudocorrelation time is much shorter than the average correlation time, i.e. the slowly decaying component is not rendered correctly by steady state measurements. Apart from this restriction the steady state anisotropy is appropriate to qualify interphases with respect to their effective viscosities. Tables 2 and 3 present some results for DPH-PA and DANS. The $\bar{\tau}_R$-values are obtained by applying eq 3 and inserting the average fluorescence lifetimes $\langle\tau_F\rangle$ from a double exponential analysis. The highest anisotropies are found in poly(methyl methacrylate) (PMMA) containing a small amount of the dimer hexamethylene-

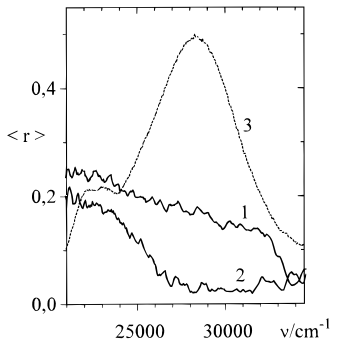

Figure 7. Fluorescence anisotropy excitation spectra of DANS−TG dispersed in water (1) and in toluene (2). For orientation, the fluorescence excitation spectrum of (2) is also presented (3).

dimethacrylate (HMDMA), which replaces the free volume of PMMA with a fairly viscous liquid. DPH and also DPH-PA approach in this medium the theoretical limit of $r_{0,max} = 0.4$, whereas DANS is far away from it, not because of higher mobility but because of the orientations of the transition dipole moments which are different in absorption and emission. From time-resolved measurements[14,30] the anisotropy maximum of DANS is $r_{0,max} = 0.3-0.32$, almost the same value as $\langle r \rangle$ in PMMA. Compared to this very rigid environment, the anisotropies are reduced in PS and even more in PEG, indicating in the latter compound high mobility with $\bar{\tau}_R$ on the order of nanoseconds.

Steady state anisotropies of the probes chemically bound to TG are unfortunately not measurable in the dry samples because one single bead is already so strongly scattering that fluorescence is completely depolarized. However, in the presence of liquids, the relative refractive index is strongly reduced so that scattering plays only a minor role on the order of $f(s) = 0.05-0.2$. Because of this remaining scattering, samples with high steady state anisotropies can be evaluated only approximately, whereas the low anisotropies give reliable values of $\bar{\tau}_R$ which are in good accordance with the swelling volumes of TG in the corresponding liquid. The mobility of DANS shows also that water is able to penetrate into TG and to solvate the PEG chains and DANS.

The steady state anisotropies of Table 2 are valid for the fluorescence maximum of DANS−TG in the corresponding liquid upon excitation into the first absorption maximum. Figure 7 shows that these values are not constant but decrease with the excitation wavenumber from the red to the blue region of the first absorption band. The high red-edge anisotropy in toluene is assigned to $(DANS)_x$ aggregates with $\bar{\tau}_R > 10$ ns, whereas the low anisotropy at the band center is due to DANS monomers with $\bar{\tau}_R \approx 1$ ns. The separation is not so evident in water since both species are rather immobile, but the anisotropy decreases systematically over the main band, indicating increasing mobility in the blue region where molecules in polar environments, i.e. with high hydration numbers, are absorbing.

DPH-PA−TG in Acetonitrile/Water Mixtures. Solvent mixtures are used in HPLC or solid state peptide and nucleotide synthesis in order to optimize the molecular distribution between stationary and mobile phase or the accessibility of the reaction centers. According to the results of Table 1, acetonitrile and water are two extreme liquids with respect to solvation and mobilization of DPH-PA chemically bound to TG. The low solvation fraction of $x_s = 0.12$ in water increases

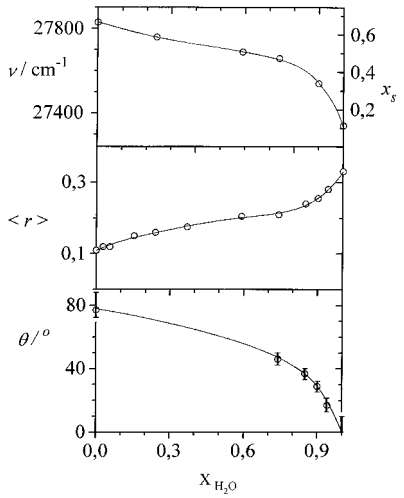

Figure 8. DPH-PA−TG in acetonitrile:water mixtures, plots versus the mole fraction of water: (upper) absorption maxima $S_0 \rightarrow S_2(0-1)$ and solvation fraction x_s, (middle) steady-state anisotropy $\langle r \rangle$ and (lower) cone semiangle θ of restricted rotation.

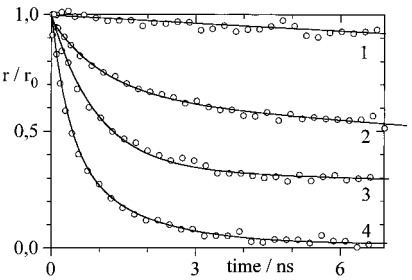

Figure 9. Fluorescence anisotropy decay curves of DPH-PA−TG dispersed in acetonitrile:water mixtures of mole fractions $X_{H_2O} = 1$ (1), $X_{H_2O} = 0.9$ (2), $X_{H_2O} = 0.74$ (3), $X_{H_2O} = 0$ (4). All curves are normalized to unity at t = 0. Circles are experimental data, and solid lines are exponential (1) and biexponential (2−4) fits.

to $x_s = 0.68$ in acetonitrile and the rotational correlation time decreases correspondingly from $\tau_R \approx 85$ ns to $\langle \tau_R \rangle \approx 0.8$ ns. In solvent mixtures, the strongest increase of x_s is observed when pure water is mixed with small amounts of acetonitrile, whereas x_s changes only very little in the region of a large excess of acetonitrile (see Figure 8, upper). The steady state anisotropies reflect the mirror image of the solvation curve (see Figure 8, middle). The high values of $\langle r \rangle$ in pure water decrease first strongly by addition of acetonitrile and then moderately in the region of excess of acetonitrile.

A selection of time-resolved anisotropy curves is presented in Figure 9. They reveal more detailed information about the mechanism of rotational depolarization in solvent mixtures. Despite the fact that the volume of TG increases in water by a factor of 2.5 relative to the dry bead, from which follows that water is the main component in the interphase system, the anisotropy decay curve in pure water shows absolutely no indication of a fast decaying process. This means that DPH must be completely immobile around its short principal axis of rotation (rotation around the long axis has no depolarizing effect since this axis is oriented parallel to the transition dipole moment of fluorescence), which can be achieved by a stiff solvation cage formed by segments of PEG and PS, but not by water. Addition of small amounts of acetonitrile induces a fast component in the anisotropy decay curve followed by a slowly decaying plateau. The amplitude A_∞ of this plateau

decreases with increasing concentration of acetonitrile. Obviously acetonitrile is able to intercalate into the polymeric solvent cage and to reduce its stiffness. As a concequence, DPH gains some degree of rotational freedom around the short axis. The simplest quantitative approximation for this type of motion is given by the wobble in cone model[31,32] in which the fluorophore can undergo free rotational diffusion within a cone of semiangle θ. This angle is related to the hight of the long-lived plateau by $2A_\infty^{1/2} = cos^2\ \theta + \cos\ \theta$. The heights were estimated graphically or, with very comparable results, by biexponential fitting. The resulting cone angles are plotted in the lower part of Fig. 8. In pure water the cone angle is very small (exact values are not obtainable because the anisotropy decays much slower than the fluorescence intensity). The angle opens widely by addition of acetonitrile and approaches 90° in pure acetonitrile. In the latter phase the stiff polymeric solvation cage has been completely replaced by a flexible solvation sphere consisiting of two parts of acetonitrile and one part of isolated polymer chains. This composition follows from the spectroscopic solvation fraction (cf. Table 1) as well as from the macroscopic composition of the interphase, where acetonitrile:TG = 2:1 per volume, and the assumption of an ideal mixture.

IV. Conclusions

The method of fluorescence probing is successfully applied to gelatinous polystyrene−poly(ethylene glycol) microbeads. This article describes how polymer/liquid interphase properties, e.g. polarizability and polarity, are investigated by chemically linked 3-(1,6-diphenyl-1,3,5-hexatrienyl)propionic acid and 1-(dimethylamino)-naphthalene-5-sulfonic acid. The extent of solvation and mobility of the probe molecules in the interphase classifies a series of liquids by their capability to penetrate into the polymeric beads. By choice of the liquid phase composition, the rotational correlation times are continuously variable from $\tau_R < 1$ ns up to $\tau_R \approx 100$ ns. In the case of high mobility, the interphase presents a reaction medium with conditions close to homogenous liquid phases.

Acknowledgment. This research is supported by the Deutsche Forschungsgemeinschaft ("Chemie in Interphasen", Li 154/41). Fluorescence anisotropy decay curves were measured at the Center for Fluorescence Spectroscopy, University of Maryland, Baltimore, MD. We thank J. R. Lakowicz for allowing us to use the instruments and H. Malak for technical assistance and helpful scientific discussions.

References and Notes

(1) Bayer, E.; Rapp, W. In *Poly(Ethylene Glycol) Chemistry: Biotechnical and Biomedical Applications*; Harris, J. M., Ed.; Plenum Press: New York, 1992.
(2) Bayer, E. *Angew. Chem. Int. Ed. Engl.* **1991**, *30*, 113−129.
(3) Hellstern, H.; Hemmasi, B. *Biol. Chem. Hoppe-Seyler* **1988**, *369*, 289−296.
(4) Bayer, E.; Albert, K.; Willisch, H.; Rapp, W.; Hemmasi, B. *Macromolecules* **1990**, *23*, 1937−1940.
(5) "Tentagel" is a trademark of Rapp Polymere GmbH, 72072 Tübingen, Germany.
(6) Allen, M. T.; Miola, L.; Whitten, D. G. *J. Am. Chem. Soc.* **1988**, *110*, 3198−3206.
(7) Pap, E. H. W.; ter Horst, J. J.; van Hoek, A.; Visser, A. J. W. G. *Biophys. Chem.* **1994**, *48*, 337−351.
(8) Saito, H.; Araiso, T.; Shirahama, H.; Koyama, T. *J. Biochem.* **1991**, *109*, 559−565.
(9) Trotter, P. J.; Storch, J. *Biochim. Biophys. Acta* **1989**, *982*, 131−139.
(10) Colles, S.; Wood, W. G.; Myers-Payne, S. C.; Igbavboa, U.; Avdulov, N. A.; Joseph, J.; Schroeder, F. *Biochemistry* **1995**, *34*, 5949−5959.
(11) Ginkel, G. v. *Appl. Fl. Techn.* **1989**, *1*, 1−8.
(12) *J. Biochem. Biophys. Meth*ods **1981**, *5*, 1−17.
(13) Miki, M.; Wahl, P.; Auchet, J.-C. *Biochemistry* **1982**, *21*, 3661−3665.
(14) Jager, W. F.; Volkers, A. A.; Neckers, D. C. *Macromolecules* **1995**, *28*, 8153−8158.
(15) Kano, K.; Ishimura, T.; Hashimoto, S. *J. Phys. Chem.* **1991**, *91*, 7839−7843.
(16) Reichhardt, C. *Chem. Rev.* **1994**, *94*, 2319−2358.
(17) Rapp, W. Dissertation, Universität Tübingen, 1985.
(18) Knight, A. E. W.; Selinger, B. K. *Aust. J. Chem* **1973**, *32*, 1−27.
(19) Cross, A. J.; Fleming, G. R. *Biophys. J.* **1984**, Vol. *46*, 45−56.
(20) Lakowicz, J. R. *Principles of Fluorescence*; Plenum Press: New York, 1983.
(21) O'Conner, D. V.; Phillips, D. *Time Dependence of Fluorescence Anisotropy*; Academic Press: New York, 1984.
(22) Cehelnik, E. D.; Cundall, R. B. *J. Phys. Chem.* **1975**, *79*, 1369−1376.
(23) Suppan, P. *J. Photochem. Photobiol. A* **1990**, *50*, 293−330.
(24) Bondarev, S. L.; Bachilo, S. M. *J. Photochem. Photobiol. A: Chem.* **1991**, *59*, 273−283.
(25) Alford, P. C.; Palmer, T. F. *J. Chem. Soc. Faraday Trans. 2* **1983**, 433−447.
(26) Brey, L. A.; Schuster, G. B.; Drickamer, H. G. *J. Chem. Phys.* **1979**, *71*, 2765.
(27) Rapp, W.; Bayer, E. *Innovations and Perspectives in Solid Phase Synthesis, Peptides, Polypeptides and Oligonucleotides*; Epton, R., Ed.; Intercept Ltd.: Andover, 1992, p 259.
(28) Holland, R. J.; Parker, E. J.; Guiney, K.; Zeld, F. R. *J. Phys. Chem.* **1995**, *99*, 11981−11988.
(29) Günther, R.; Oelkrug, D.; Rettig, W. *J. Phys. Chem.* **1993**, *97*, 8512−8518.
(30) Yguerabide, J.; Epstein, H. F.; Stryer, L. *J. Mol. Biol.* **1970**, *51*, 573−590.
(31) Steiner, R. In *Topics in Fluorescence Spectroscopy, Principles*; Lakowicz, J. R., Ed.; Plenum Press: New York, 1991.
(32) Kinosita, K., Jr.; Kawato, S.; Ikegami, A. *Biophys. J.* **1977**, *20*, 289−305.

MA960558K